Carbon 130 (2018) 410–415

Contents lists available at ScienceDirect

Carbon

journal homepage: www.elsevier.com/locate/carbon

Carbon addition lowers initiation and iodine release temperatures from iodine oxide-based biocidal energetic materials

Tao Wu [a], Xizheng Wang [a], Jeffery B. DeLisio [a], Scott Holdren [a], Michael R. Zachariah [a, b, *]

[a] Department of Chemistry and Biochemistry, University of Maryland, College Park, MD 20742, USA
[b] Department of Chemical and Biomolecular Engineering, University of Maryland, College Park, MD 20742, USA

ARTICLE INFO

Article history:
Received 8 September 2017
Received in revised form
12 December 2017
Accepted 1 January 2018
Available online 9 January 2018

ABSTRACT

Iodine oxides are of significant interest as strong oxidizers in energetic formulation that also operate as iodine release agents for neutralization of spores using strong thermal pulses. In this paper incorporation of carbon black (CB) as the main fuel or additive into iodine oxides-based energetic materials are shown to lower both initiation and iodine release temperatures compared to those of Al/iodine oxides and Ta/iodine oxides thermites. Those lowering effects were triggered by a condensed phase CB-iodine oxides reaction explored by high heating rate time-resolved temperature-jump time-of-flight mass spectrometry and low heating rate thermogravimetric analysis/differential scanning calorimetry results. We observe that other carbon allotropes, such as carbon nanotubes and functionalized graphene sheets, also feature the similar effect as CB. Fourier transform infrared spectroscopy analysis shows that the presence of CB lowered the bond energy of iodine oxide on the surface to trigger the CB-iodine oxide initiation at a relatively lower temperature.

1. Introduction

Developing new energetic materials with high efficiency neutralization of biological warfare agents has gained increased attention due to the increased threat of bioterrorism [1–5]. Preliminary laboratory studies have suggested that an ideal neutralization process should generate not only a high temperature, but also release a long-lasting biocidal agent [6–12]. The main limitation of conventional energetic materials is low neutralization efficiency since the thermal neutralization mechanism is dominant in this case, with the lack of effective biocidal agent release [6]. Therefore, it has been proposed that simultaneously delivering a rapid thermal pulse with a remnant biocidal agent would prolong the exposure time and improve the inactivation process [13].

Halogen-containing energetic materials have shown the most promise because of their excellent biocidal properties [14], compared to other biological energetic materials [15–17]. Among all halogens, iodine stands out owing to its strong neutralization effect. Different methods have been reported for incorporating elemental iodine into energetic materials [14,18–20]. For instance, Dreizin et al. employed mechanically alloyed aluminum-iodine composites as a fuel in energetic formulations and the initiation and combustion tests in air indicated that higher iodine concentration lowers initiation temperatures and the combustion temperatures were not substantially diminished [12]. They also found improvements in terms of pressurization rate and maximum pressure at constant volume with 15 wt% and 20 wt% of I_2 [12]. Furthermore, an effective inactivation of aerosolized spores has been achieved using Al/I_2 and Al/B/I_2 composites with 15–20 wt% of iodine [14]. Another efficient method is to use iodine-containing compounds as an oxidizer, particularly iodine oxides/iodic acids.

Among all the iodine oxides/iodic acids (I_2O_5, I_4O_9, HI_3O_8, HIO_3, H_5IO_6, etc [21–23]), I_2O_5 is the most studied in thermite systems [24–28] due to its relatively high iodine content (~76% iodine mass fraction). In these studies, aluminum particles with different sizes were chosen as the fuel due to its high reaction enthalpy, thermal conductivity and availability. With reported propagation velocities of up to ~2000 m/s for loose ball-milled nano-aluminum and nano-scaled I_2O_5 (~10 nm) [27], I_2O_5 shows its high potential in aluminum-based thermites as an extremely aggressive oxidizer. Constant volume combustion tests also show nano-Al/micro-I_2O_5 outperforms traditional aluminum-based thermites such as Al/CuO and Al/Fe_2O_3 [28].

* Corresponding author. Department of Chemistry and Biochemistry and Department of Chemical and Biomolecular Engineering, University of Maryland, College Park, MD 20742, USA.
E-mail address: mrz@umd.edu (M.R. Zachariah).

https://doi.org/10.1016/j.carbon.2018.01.001
0008-6223/

Aluminum has a passivating alumina shell that stabilizes the material at ambient conditions. However, once the aluminum core is heated near the melting temperature, obtaining sufficient mobility, it can diffuse through the oxide shell and interact with any available oxidizer ultimately leading to initiation [29]. However, iodine oxide releases O_2 at a relatively low temperature (~450 C) which is well below the Al melting point, where reaction is most advantaged [30]. To explore the fuel melting aspect of initiation, we have also used tantalum as a fuel since it has a much higher melting point (~3000 °C) than Al (660 °C), and thus would not melt at the point of initiation. However, the immobile tantalum core will not react with iodine oxide until some cracks appeared in the Ta_2O_5 shell upon heating (higher than 500 °C) due to the amorphous to crystalline phase change of the oxide shell [31]. Those cracks serve as a low resistance pathway for the oxygen to react with the tantalum core [31].

In this work, we employed carbon as a fuel to better interpret the initiation process of iodine oxide-based energetic materials since it has a high melting point (3550 °C) and no passivating shell. Therefore, there will be direct contact between the fuel and oxidizer enabling further understanding of the initiation process. Time-resolved temperature-jump time-of-flight mass spectrometry was used to study the initial events of bare oxidizers or carbon/iodine oxides thermites under rapid heating rates, enabling us to probe the reaction process on a time scale close to that of a combustion event. Slow heating rate thermogravimetric analysis and differential scanning calorimetry in an argon environment was also employed to further probe the reaction mechanism. Both methods indicate that carbon black (CB) and other carbon allotropes, such as functionalized graphene sheets and carbon nanotubes, can lower the iodine release temperature from iodine oxides such as I_2O_5, HIO_3 and HI_3O_8, via a condensed phase reaction mechanism. More importantly, we also found that CB as an additive with only 3 wt% can also significantly lower the initiation and iodine release temperatures for both Al/iodine oxides and Ta/iodine oxides thermites, indicating the potential use of CB in biocidal applications. In addition, Fourier transform infrared spectroscopy analysis was employed to examine the structural changes, specifically how the vibrations of I_2O_5 are affected by the addition of carbon black. The result implies that the presence of carbon black lowered the bond energy of iodine oxide on the surface and therefore triggered this condensed phase reaction.

2. Experimental

2.1. Materials

The aluminum nanopowders (Al) (Alex, ~80 nm) were purchased from Novacentrix. The active Al was 81% by mass, determined by thermogravimetric analysis. Nano-tantalum powders (<50 nm, Ta) were purchased from Global Advanced Metals. Nano-sized carbon black (~50 nm, CB) was obtained from Cabot Corporation. Multi-wall carbon nanotubes and iodine pentoxide (I_2O_5) purchased from Sigma-Aldrich were directly used as received. Functionalized graphene sheets (FGS) with C:O molar ratio of 15 and 60 were obtained from Aksay et al. [32] and labeled as FGS_{15} and FGS_{60}, respectively. All the other chemicals were of analytical grade and used as purchased without further treatment. HI_3O_8 was prepared via thermal treatment of commercial HIO_3 at ~180 °C for 30 min.

2.2. Preparation of thermites

Aluminum, tantalum or CB was stoichiometrically mixed with I_2O_5, HIO_3 and HI_3O_8 based on the following equations, respectively, in hexane followed by 30 min of sonication.

$$3C + 2HIO_3 \rightarrow 3I_2 + H_2 + 3CO_2$$

$$8C + 2HI_3O_8 \rightarrow 3I_2 + H_2 + 8CO_2$$

$$5C + 2I_2O_5 \rightarrow 2I_2 + 5CO_2$$

$$4Al + 2HIO_3 \rightarrow I_2 + 2Al_2O_3 + H_2$$

$$32Al + 6HI_3O_8 \rightarrow 9I_2 + 16Al_2O_3 + 3H_2$$

$$10Al + 3I_2O_5 \rightarrow 3I_2 + 5Al_2O_3$$

After room temperature evaporation of the solvent in a desiccator, the solid thermite powders were used. To show the morphology of the thermites, as an example, the SEM images of CB/Ta/HI_3O_8 along with Ta/HI_3O_8 and HI_3O_8 are shown in Fig. S1. The fact that fuel (CB, Ta) nanoparticles were well distributed on the surface of HI_3O_8 indicates a good mixing of fuel and oxidizer.

2.3. Temperature-jump time-of-flight mass spectrometry-(Jump/TOFMS) measurement and high-speed imaging

The decomposition of oxide particles was investigated using a T-Jump/TOFMS [6]. Typically, a ~1 cm long platinum wire (76 μm in width) with a thin layer coating of oxidizer sample was rapidly joule-heated to about 1200 °C by a 3 ms pulse at a heating rate of $5 \times \sim 10^5$ °C/s. The current and voltage signals were recorded, and the temporal temperature of the wire was measured according to the Callendar–Van Dusen equation [29]. However, the sample temperature can be different than the wire temperature, and we are only able to directly measure the wire temperature by this method. To address this concern, we have previously developed a heat transfer model to estimate the true sample temperature during the heating event [33,34]. The major conclusion from this quantitative model is that the characteristic heating time of nanoparticles on the wire is sufficiently fast, that even though we are using a high heating rate, the nanoparticles on the wire are expected to be essentially at the wire temperature (± 5 °C). Therefore, initiation/ignition temperatures of the materials in contact with the wire is equal to the wire temperature within any experimental and practical effect. Adding a material with a higher thermal conductivity such as carbon would only improve the situation. The temperature of the wire corresponding to the initial release of O_2 or iodine was regarded as the O_2 or iodine release temperature. Mass spectra were measured every 0.1 ms. The detailed experimental set-up is given in our previous papers [6,29].

To identify the point of initiation, a high-speed camera (Vision Research Phantom v12.0) was employed to record the combustion on the wire during heating. Initiation temperatures of thermite reactions in vacuum were measured from the correlation of optical emission from high speed imaging and temporal temperature of the wire, and were further analyzed in combination with the temporal mass spectra. Each measurement was repeated 3 times.

2.4. Thermogravimetric analysis/differential scanning calorimetry (TGA/DSC) measurement

Thermogravimetric analysis and Differential Scanning Calorimetry were conducted using an SDT Q600 (TA instruments). The measurement was performed under a 100 mL min^{-1} argon flow with ~1.0 mg samples placed into an alumina pan and heated from room temperature up to 550 °C (or higher temperature) at a rate of

5 °C/min.

2.5. Fourier transform infrared spectroscopy (FTIR) analysis

Attenuated total reflection (ATR) FTIR spectra of I_2O_5 samples with and without CB were collected using a Nicolet iS-50R spectrometer equipped with a room temperature deuterated triglycine sulfate (DTGS) detector FTIR spectroscopy. A Thermo Scientific Smart iTX accessory was installed to collect the ATR spectra shown here at 4 cm^{-1}resolution and averaged over 25 scans.

3. Results and discussion

To investigate the performance of iodine oxides/iodic acids as oxidizers in thermite systems, we have previously employed Al and Ta as fuels. However, both aluminum and tantalum have an oxide shell, which to some extent restricted our understanding on how those thermites react during initiation [35], and thus motivated the use of carbon. Commercial iodine pentoxide was first examined because it is the most extensively studied and can be obtained easily [36].

T-Jump/TOFMS was employed to study the initial events of bare oxidizers or thermites under rapid heating [37]. We plot in Fig. 1 both the iodine and oxygen release temperatures vs. the reaction initiation temperature. Different initiation temperatures were obtained for thermites with different fuels including Al, Ta and CB. We have previously argued that the initiation of Al-based and Ta-based thermites is dominated by the melting of aluminum and the phase change of the Ta_2O_5 shell, respectively [35]. As to CB, the initiation temperature of CB/I_2O_5 is ~330 °C (determined from release of CO_2 product since there is virtually no optical signature of initiation), and more than 100 °C lower than the iodine release temperature from the neat I_2O_5, which implies a condensed phase reaction mechanism may be dominant here.

Ignition by its nature is essentially the point where self-heating by exothermic reaction exceeds heat loss and product formation occurs. It should be noted that the light emission of metal based thermites aligns well with the product release profile based on our previous work [29]. One major conclusion from this paper is that the product formation determined by mass spectrometry correlates well with the temperature at which light emission begins. Therefore, ignition/initiation in these experiments is defined at the point of CO_2 production for C-based thermites (Fig. S2) and the light emission of Al/Ta-based thermites.

To understand the relationship between iodine release and initiation, we plotted iodine release temperatures vs initiation temperatures in Fig. 2. The dotted red line represents the iodine/O_2 release temperatures (~450 °C) from neat I_2O_5 obtained through a high heating method. Note that, the y-axis in Fig. 2 is the iodine/O_2 release temperature of the fuel/I_2O_5 mixture; however, the y-axis in Fig. 1 is the iodine/O_2 release temperature of the neat I_2O_5. Since CB/I_2O_5 ignition was initiated at a very low temperature, 3 wt% CB was introduced into both Al/I_2O_5 and Ta/I_2O_5 systems to investigate the effect of CB as an additive.

Results in Fig. 2 shows that the initiation temperature is correlated with the iodine release temperature for all cases except for Al/I_2O_5 in which its initiation was controlled by the mobilization of the aluminum core. When aluminum is employed as the fuel, iodine release is actually delayed to a significantly higher temperature compared with neat I_2O_5 (550 vs. 450 °C). This delay might be caused by the interaction between the alumina shell and I_2O_5, which to some extent stabilizes I_2O_5 and therefore delays its decomposition. Similar effects of halogen interactions have been reported in previous studies [26,38].

Fig. 2 also shows that addition of just 3 wt% CB into Al/I_2O_5 system, not only lowers the iodine release temperature but also the initiation temperature. The incorporated CB offsets the influence of aluminum on the iodine release from I_2O_5 and makes it behave like that of the bare oxidizer. As to why initiation seems not limited by the melting point of Al: the condensed phase reaction of CB/I_2O_5 is initiated first and presumably the energy generated kicks the temperature above the point of making the Al core mobile. Thus, addition of CB lowers the initiation temperature of an aluminum based thermite.

As a comparison, $CB_{3wt\%}/I_2O_5$ (non-stoichiometric) shows a lower initiation and iodine release temperatures than $CB_{3wt\%}$/Al/I_2O_5, which indicates the presence of aluminum inhibits the condensed phase reaction of CB/I_2O_5 and therefore delays the iodine release from I_2O_5. On the other hand, with only 3 wt% addition of CB, the iodine release temperature of I_2O_5 was brought lower by about 50 °C compared to the neat I_2O_5, which indicates that the condensed phase CB/I_2O_5 reaction occurred before the I_2O_5

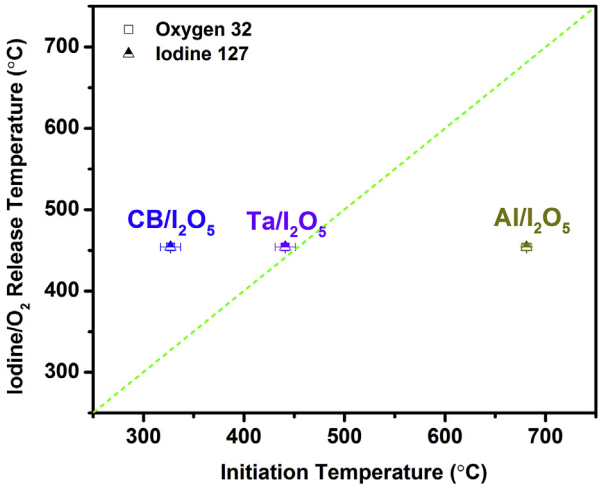

Fig. 1. Release temperature of I and O_2 from neat I_2O_5 vs. initiation temperature of corresponding Al-based, Ta-based and CB-based thermites under vacuum. Error bars represent two replicates. The diagonal dashed line would imply a perfect correlation between initiation and release temperature. (A colour version of this figure can be viewed online.)

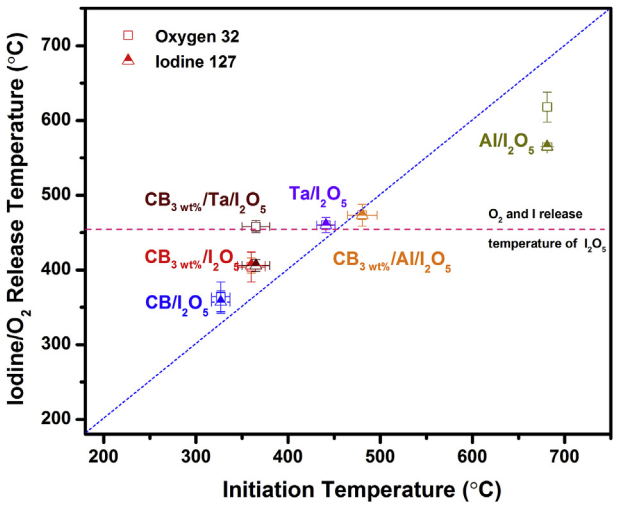

Fig. 2. Release temperatures of iodine/oxygen vs. initiation temperatures of different thermites. (A colour version of this figure can be viewed online.)

decomposition. Furthermore, the addition of 3 wt% CB into Ta/I_2O_5 system also bring both iodine release and initiation to lower temperatures, indicating the general effect of CB additive on different fuel/I_2O_5 systems. In addition, time resolved images of $CB_{3wt\%}$/Al/I_2O_5 and $CB_{3wt\%}$/Ta/I_2O_5 thermite reactions during rapid heating under vacuum were captured using a high-speed camera and are shown in Fig. S3. In contrast to $CB_{3wt\%}$/Al/I_2O_5, the $CB_{3wt\%}$/Ta/I_2O_5 reaction is much more vigorous with strong light emission.

In fact, similar results (Fig. S4) were also obtained for HI_3O_8-based or HIO_3-based thermites indicating the general effect of CB on iodine oxides/iodic acids.

We now turn to mechanistic effects, which we limit to the CB/I_2O_5 reaction mechanism since the other oxidizers showed similar behavior.

To explore the CB/I_2O_5 reaction further, time-resolved T-Jump mass spectra of I_2O_5 and CB/I_2O_5 were obtained and shown in Fig. 3. For neat I_2O_5, above the decomposition temperature (>1.1 ms, 470 °C), O_2^+ and I^+ are detected in addition to IO^+, IO_2^+, I_2^+, and I_2O^+, which is consistent with our previous result of HI_3O_8. Since IO^+ and IO_2^+ were reported previously as the primary species of iodic acid, we conclude that the commercial I_2O_5 is partially hydrated to form HI_3O_8. In fact, the XRD and TGA/DSC results (Fig. S5) of commercial I_2O_5 also prove it is ~80% hydrated to HI_3O_8 [35,36]. For CB/I_2O_5, both the disappearance of the O_2^+ peak and the appearance of a CO_2^+ peak prove CB reacted with I_2O_5. The time-resolved mass spectra of bare CB (Fig. S6) clearly eliminates the possibility that the CO_2^+ peak is from CB. The new CO^+ peak is either a fragment of CO_2 or a product of incomplete reaction of CB/I_2O_5 energetic composite. Considering both facts that the reaction is extremely fast (less than several milliseconds) and the formed O_2 could rapidly escape the reaction interface at very low pressure, the partially incomplete reaction between the fuel and oxidizer is not a surprise.

Fig. 3 also shows that CB/I_2O_5 released iodine at ~360 °C, which occurred slightly later than its initiation temperature (~340 °C), indicating a condensed phase reaction mechanism was involved here. More importantly, the onset release temperature of iodine from CB/I_2O_5 is about 100 °C lower than that of neat I_2O_5, which is probably due to that the condensed phase reaction of CB extracts oxygen from I_2O_5, and thus promoting a quicker release of iodine.

Slow heating rate TGA in argon is shown in Fig. 4. Neat I_2O_5 shows one minor weight loss at around 210 °C that corresponds to the dehydration of HI_3O_8 and another major weight loss at around 370 °C that results from the decomposition of I_2O_5. The DSC curve of I_2O_5 shows that both steps are endothermic (black curve in Fig. S7).

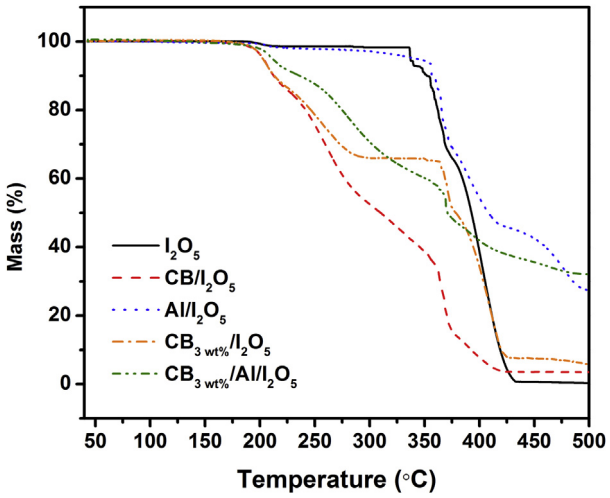

Fig. 4. TGA results of neat I_2O_5, CB/I_2O_5, Al/I_2O_5 and $CB_{3\ wt\%}$/Al/I_2O_5 thermites. (A colour version of this figure can be viewed online.)

When CB was mixed with I_2O_5 (red curve in Fig. 4) the onset decomposition temperature is 140 °C lower than that of neat I_2O_5. In addition, the DSC (red curve in Fig. S7) shows an exotherm around 250 °C presumably from reaction between CB and I_2O_5. Even with only 3 wt% of CB, the TGA curve of I_2O_5 follows the same kinetics as CB/I_2O_5 at temperatures below 250 °C. However, as temperature increases (250 < T < 300 °C), the reaction effectively stops until it reaches the neat I_2O_5 condition resuming decomposition at a rate the same as neat I_2O_5. In fact, the actual weight loss of $CB_{3wt\%}$/I_2O_5 at 300 °C, ~35%, is very close the theoretical weight loss ~37% based on the reaction of 3 wt% CB and I_2O_5 (accounted for the 80% hydration HI_3O_8 specie).

The unchanged TGA result of Al/I_2O_5 compared with that of I_2O_5 indicates that aluminum does not pose any significant influence on the decomposition of I_2O_5 at low heating rates, which is quite different from the T-jump/TOFMS experiment in which the presence of aluminum delays the iodine release of I_2O_5. Moreover, for

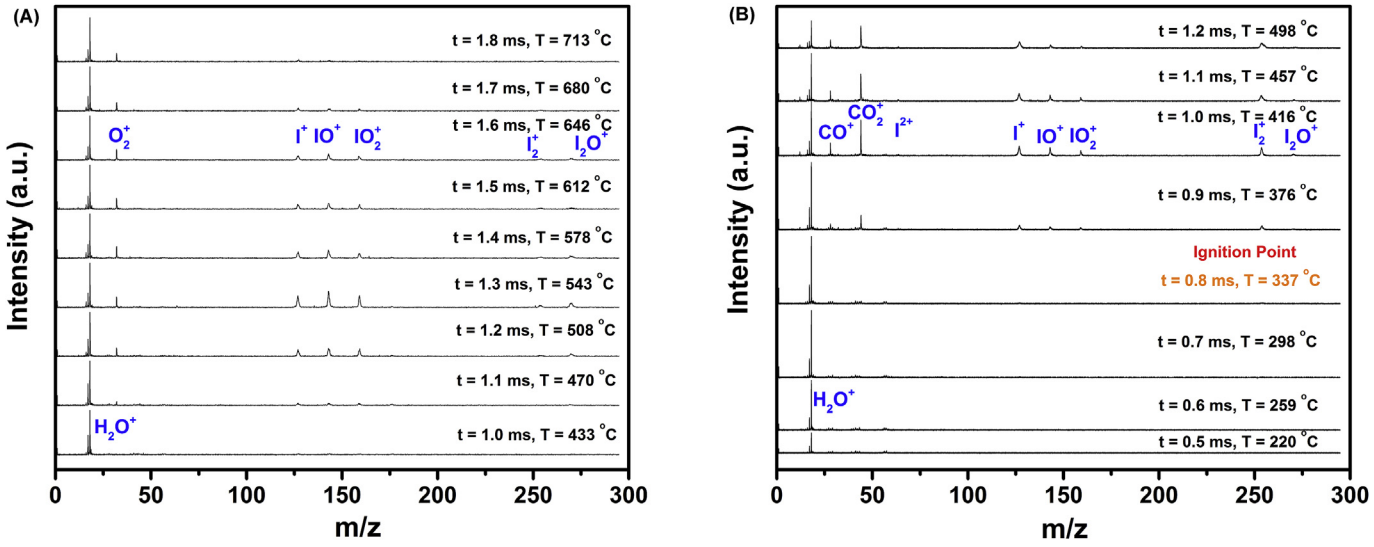

Fig. 3. Time-resolved mass spectra of I_2O_5 (A) and CB/I_2O_5 (B). (A colour version of this figure can be viewed online.)

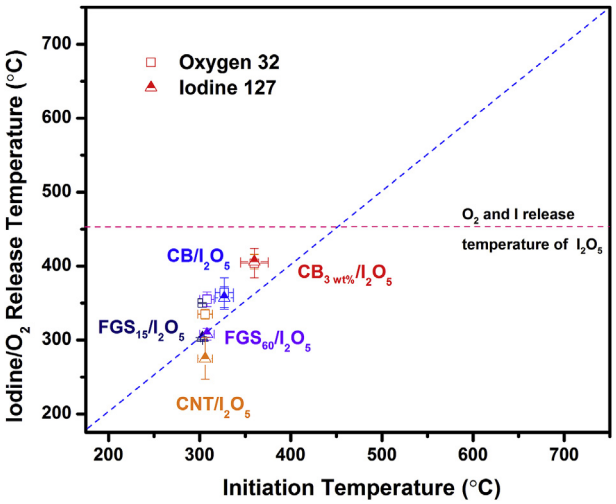

Fig. 5. The relation between iodine/oxygen release temperatures and initiation temperatures of thermites employing carbon allotropes as the fuel. (A colour version of this figure can be viewed online.)

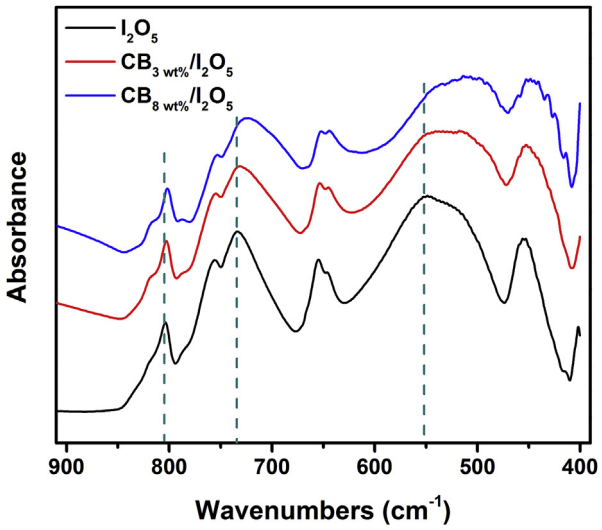

Fig. 6. ATR-FTIR spectra of bare I_2O_5, $CB_{3wt\%}/I_2O_5$ and $CB_{8wt\%}/I_2O_5$ at room temperature showing I-O bond red-shift upon addition of CB. (A colour version of this figure can be viewed online.)

$CB_{3wt\%}/Al/I_2O_5$, the decomposition started at a temperature very close to that of CB/I_2O_5, thus aluminum does not influence the CB/I_2O_5 reaction at a low heating rate and again differs from the T-jump/TOFMS experiment.

The TGA curve (Fig. S8A) of Ta/I_2O_5 starts decreasing at a lower temperature than that of bare I_2O_5, which suggests Ta/I_2O_5 reaction was probably initiated prior to I_2O_5 decomposition at low heating rate and thus causing the weight loss. The TGA/DSC of nTa in O_2 at a heating rate of 20 °C/min (Fig. S9) shows oxidation is a one step process beginning at ~300 °C and finishing at ~500 °C, indicating that gaseous O_2 can diffuse through the Ta_2O_5. Thus, the Ta/I_2O_5 reaction was probably initiated by the interaction between the Ta core and the oxidizer I_2O_5 following a condensed phase reaction mechanism. The 3 wt% addition CB into Ta/I_2O_5 system, decreases the onset decomposition temperature, but the kinetics were found to be faster (Fig. S8A) and a small exotherm was observed (Fig. S8B).

Additional carbon allotropes including CNT and FGS were evaluated by stoichiometrically mixing with I_2O_5. Fig. 5 shows the relation between iodine release temperatures and initiation temperatures of those energetic composites employing carbon allotropes as the fuel from T-Jump mass spectrometry. The horizontal dotted red line represents the oxygen and iodine release temperatures of neat I_2O_5, and the dotted blue line would refer to the perfect correlation between iodine release and the onset reaction temperature. For all samples, the initiation temperatures are either lower to or the same as the corresponding iodine release temperatures and the iodine release temperature is lower than bare I_2O_5. All four stoichiometric thermites employing FGS_{15}, FGS_{60}, CNT or CB as the fuel initiated almost at the same temperature ~310 °C, implying that the different properties among those carbon materials [39–42] appear to have no significant effect on initiation. We also note that above a threshold level of carbon the ignition temperature is not affected. So, 3% and 8% of CB addition have essentially the same ignition temperature. Additionally, the low heating rate TGA/DSC results (Fig. S10) show similar onset decomposition temperatures and exothermic peaks as to CB/I_2O_5, which are in consistent with the initiation results.

Since we conclude that surface reaction is clearly playing a significant role, FTIR attenuated total reflection (ATR, surface) and transmission measurements (KBr pellet) were both employed to deduce any structure changes just prior to reaction [43]. FTIR-ATR spectra of bare I_2O_5, $CB_{3wt\%}/I_2O_5$ and stoichiometric CB/I_2O_5 at room temperature, is shown in Fig. 6. The spectra show a steady red-shift (to lower wavenumbers) with increasing CB content. For clarity, the stoichiometric CB/I_2O_5 is labeled as $CB_{8wt\%}/I_2O_5$. The redshifts indicate weaker iodine-oxygen bonds due to the presence of CB. In addition, no new peak is detected with CB-added samples which suggests no new carbon-iodine or carbon-oxide bonds are formed between CB and iodine oxide. Transmission FTIR-KBr pellet spectra (Fig. S11) show no discernible changes in the spectra. Keeping in mind that the ATR is a surface sensitive technique while the KBr pellet method is a bulk technique we can conclude that the surface of I_2O_5 particles even under room temperature conditions is affected by CB in a manner to enable a lower decomposition temperature.

4. Conclusions

In this paper, we employed carbon (CB, CNT and FGS) as both a fuel and as an additive to aluminum and tantalum fuels to study the influence of a fuel without nascent oxide shell on initiation of iodine oxide-based thermites. We found that the initiation temperature of CB/I_2O_5 is much lower than the initiation temperature of Al/I_2O_5 and Ta/I_2O_5. When CB is used as an additive to other fuels we observe a decrease in the overall initiation temperature and a lowering of the iodine release temperature to below that of the nascent oxidizer. Other carbon allotropes showed similar results. FTIR analysis indicated at CB lowered the iodine-oxygen bond energy of I_2O_5 on the surface and thus triggered this condensed phase reaction. These results indicate that CB can be employed as an additive to any metal fuel as a means to lower both the initiation and iodine release temperature.

Acknowledgements

Support for this work comes from the Defense Threat Reduction Agency.

Appendix A. Supplementary data

Supplementary data related to this article can be found at https://doi.org/10.1016/j.carbon.2018.01.001.

References

[1] E.R. Blatchley, A. Meeusen, A.I. Aronson, L. Brewster, Inactivation of Bacillus spores by ultraviolet or gamma radiation, J. Environ. Eng-Asce 131 (9) (2005) 1245–1252.

[2] K.T. Sullivan, C.W. Wu, N.W. Piekiel, K. Gaskell, M.R. Zachariah, Synthesis and reactivity of nano-Ag2O as an oxidizer for energetic systems yielding antimicrobial products, Combust. Flame 160 (2) (2013) 438–446.

[3] M. Schoenitz, T.S. Ward, E.L. Dreizin, Fully dense nano-composite energetic powders prepared by arrested reactive milling, Proc. Combust. Inst. 30 (2005) 2071–2078.

[4] G.J. Feng, Z.R. Li, Z. Zhou, Y. Wang, Joining of C-f/Al composites and TiAl intermetallics by laser-induced self-propagating high-temperature synthesis using the Ni-Al-Zr interlayer, Mater. Des. 110 (2016) 130–137.

[5] K. Zhang, C. Rossi, G.A.A. Rodriguez, C. Tenailleau, P. Alphonse, Development of a nano-Al/CuO based energetic material on silicon substrate, Appl. Phys. Lett. 91 (11) (2007).

[6] K.T. Sullivan, N.W. Piekiel, S. Chowdhury, C. Wu, M.R. Zachariah, C.E. Johnson, Ignition and combustion characteristics of nanoscale Al/AgIO3: a potential energetic biocidal system, Combust. Sci. Technol. 183 (3) (2011) 285–302.

[7] W.B. Zhou, M.W. Orr, V.T. Lee, M.R. Zachariah, Synergistic effects of ultrafast heating and gaseous chlorine on the neutralization of bacterial spores, Chem. Eng. Sci. 144 (2016) 39–47.

[8] W. Zhou, M.W. Orr, G. Jian, S.K. Watt, V.T. Lee, M.R. Zachariah, Inactivation of bacterial spores subjected to sub-second thermal stress, Chem. Eng. J. 279 (2015) 578–588.

[9] F.T. Tabit, E. Buys, The effects of wet heat treatment on the structural and chemical components of Bacillus sporothermodurans spores, Int. J. Food Microbiol. 140 (2–3) (2010) 207–213.

[10] S.S. Zhang, M. Schoenitz, E.L. Dreizin, Mechanically alloyed Al-I composite materials, J. Phys. Chem. Solid. 71 (9) (2010) 1213–1220.

[11] S.S. Zhang, M. Schoenitz, E.L. Dreizin, Iodine release, oxidation, and ignition of mechanically alloyed Al-I composites, J. Phys. Chem. C 114 (46) (2010) 19653–19659.

[12] S.S. Zhang, C. Badiola, M. Schoenitz, E.L. Dreizin, Oxidation, ignition, and combustion of Al center dot I-2 composite powders, Combust. Flame 159 (5) (2012) 1980–1986.

[13] H. Wang, G. Jian, W. Zhou, J.B. DeLisio, V.T. Lee, M.R. Zachariah, Metal iodate-based energetic composites and their combustion and biocidal performance, Acs Appl. Mater. Inter. 7 (31) (2015) 17363–17370.

[14] Y. Aly, S. Zhang, M. Schoenitz, V.K. Hoffmann, E.L. Dreizin, M. Yermakov, R. Indugula, S.A. Grinshpun, Iodine-containing aluminum-based fuels for inactivation of bioaerosols, Combust. Flame 161 (1) (2014) 303–310.

[15] C.E. Johnson, K.T. Higa, Iodine-rich biocidal reactive materials, in: MRS Proceedings 1521, 2013.

[16] O. Mulamba, E.M. Hunt, M.L. Pantoya, Neutralizing bacterial spores using halogenated energetic reactions, Biotechnol. Bioproc. E 18 (5) (2013) 918–925.

[17] C.L. He, J.H. Zhang, J.M. Shreeve, Dense iodine-rich compounds with low detonation pressures as biocidal agents, Chem. Eur J. 19 (23) (2013) 7503–7509.

[18] T. Wu, A. SyBing, X.Z. Wang, M.R. Zachariah, Aerosol synthesis of phase pure iodine/iodic biocide microparticles, J. Mater. Res. 32 (4) (2017) 890–896.

[19] H.Y. Wang, J.B. DeLisio, G.Q. Jian, W.B. Zhou, M.R. Zachariah, Electrospray formation and combustion characteristics of iodine-containing Al/CuO nanothermite microparticles, Combust. Flame 162 (7) (2015) 2823–2829.

[20] S.E. Guerrero, E.L. Dreizin, E. Shafirovich, Combustion of thermite mixtures based on mechanically alloyed aluminum-iodine material, Combust. Flame 164 (2016) 164–166.

[21] B.K. Little, S.B. Emery, J.C. Nittinger, R.C. Fantasia, C.M. Lindsay, Physiochemical characterization of Iodine(V) oxide, Part 1: Hydration rates, Propell Explos Pyrot 40 (4) (2015) 595–603.

[22] A. Fischer, Redetermination of HI3O8, an adduct of formula HIO3 center dot I2O5, Acta Crystallogr. E 61 (2005) I278–I279.

[23] A. Wikjord, P. Taylor, D. Torgerson, L. Hachkowski, Thermal-behavior of corona-precipitated iodine oxides, Thermochim. Acta 36 (3) (1980) 367–375.

[24] K.S. Martirosyan, Nanoenergetic Gas-Generators: principles and applications, J. Mater. Chem. 21 (26) (2011) 9400–9405.

[25] B.K. Little, E.J. Welle, S.B. Emery, M.B. Bogle, V.L. Ashley, A.M. Schrand, C.M. Lindsay, Chemical dynamics of nano-aluminum/iodine (V) oxide, J. Phys. Conf. 500 (2014).

[26] C. Farley, M. Pantoya, Reaction kinetics of nanometric aluminum and iodine pentoxide, J. Therm. Anal. Calorim. 102 (2) (2010) 609–613.

[27] E.L. Dreizin, M. Schoenitz, Correlating ignition mechanisms of aluminum-based reactive materials with thermoanalytical measurements, Prog. Energy Combust. 50 (2015) 81–105.

[28] G. Jian, S. Chowdhury, J. Feng, M.R. Zachariah, The ignition and combustion study of nano-al and iodine pentoxide thermite, in: 8th U. S. National Combustion Meeting, Western States Section of the Combustion Institute, Utah, 2013, pp. 1–13.

[29] G. Jian, N.W. Piekiel, M.R. Zachariah, Time-resolved mass spectrometry of Nano-Al and nano-Al/CuO thermite under rapid heating: a mechanistic study, J. Phys. Chem. C 116 (51) (2012) 26881–26887.

[30] G.Q. Jian, S. Chowdhury, K. Sullivan, M.R. Zachariah, Nanothermite reactions: is gas phase oxygen generation from the oxygen carrier an essential prerequisite to ignition? Combust. Flame 160 (2) (2013) 432–437.

[31] J.B. DeLisio, G.C. Egan, S.-C. Liou, W.-A. Chiou, M.R. Zachariah, Probing the oxidation mechanism of Ta nanoparticles via in-situ and ex-situ ultra-fast heating TEM/STEM, Microsc. Microanal. 22 (S3) (2016) 780–781.

[32] C. Punckt, M.A. Pope, Y.F.M. Liu, I.A. Aksay, Structure-dependent electrochemistry of reduced graphene oxide monolayers, J. Electrochem. Soc. 163 (7) (2016) H491–H498.

[33] L. Zhou, Development of Ion-mobility and Mass Spectrometry for Probing the Reactivity of Nanoparticles and Nanocomposites, University of Maryland, College Park, Md, 2009.

[34] S. Chowdhury, K. Sullivan, N. Piekiel, L. Zhou, M.R. Zachariah, Diffusive vs explosive reaction at the nanoscale, J. Phys. Chem. C 114 (20) (2010) 9191–9195.

[35] T. Wu, X. Wang, J.B. DeLisio, H. Wang, M.R. Zachariah, Performance of iodine oxides/iodic acids as oxidizers in thermite systems, Combust. Flame (2017). In press.

[36] D.K. Smith, K. Hill, M.L. Pantoya, J.S. Parkey, M. Kesmez, Reactive characterization of anhydrous iodine (v) oxide (I2O5) with aluminum: amorphous versus crystalline microstructures, Thermochim. Acta 641 (2016) 55–62.

[37] X.Z. Wang, W.B. Zhou, J.B. DeLisio, G.C. Egan, M.R. Zachariah, Doped delta-bismuth oxides to investigate oxygen ion transport as a metric for condensed phase thermite ignition, Phys. Chem. Chem. Phys. 19 (20) (2017) 12749–12758.

[38] J.B. DeLisio, X.L. Hu, T. Wu, G.C. Egan, G. Young, M.R. Zachariah, Probing the reaction mechanism of aluminum/poly(vinylidene fluoride) composites, J. Phys. Chem. B 120 (24) (2016) 5534–5542.

[39] T. Wu, M.X. Chen, L. Zhang, X.Y. Xu, Y. Liu, J. Yan, W. Wang, J.P. Gao, Three-dimensional graphene-based aerogels prepared by a self-assembly process and its excellent catalytic and absorbing performance, J. Mater. Chem. 1 (26) (2013) 7612–7621.

[40] B. Lian, J. Deng, G. Leslie, H. Bustamante, V. Sahajwalla, Y. Nishina, R.K. Joshi, Surfactant modified graphene oxide laminates for filtration, Carbon 116 (2017) 240–245.

[41] D.M. Hu, W.B. Gong, J.T. Di, D. Li, R. Li, W.B. Lu, B.H. Gu, B.Z. Sun, Q.W. Li, Strong graphene-interlayered carbon nanotube films with high thermal conductivity, Carbon 118 (2017) 659–665.

[42] S. Kim, M. Jang, M. Park, N.H. Park, S.Y. Ju, A self-assembled flavin protective coating enhances the oxidative thermal stability of multi-walled carbon nanotubes, Carbon 117 (2017) 220–227.

[43] P.M. Sherwood, J.J. Turner, Vibrational spectra of compounds in iodine pentoxide-water system and sodium iodate, Spectrochim Acta a-M A 26 (10) (1970), 1975-&.